



HAL
open science

Source follower noise limitations in CMOS active pixel sensors

Keith Findlater, Jérôme Vaillant, Donald Baxter, Christine Augier, Didier Herault, Robert Henderson, Jed Hurwitz, Lindsay A. Grant, Jean-Marc Volle

► To cite this version:

Keith Findlater, Jérôme Vaillant, Donald Baxter, Christine Augier, Didier Herault, et al.. Source follower noise limitations in CMOS active pixel sensors. *Optical Systems Design*, SPIE, Feb 2004, St. Etienne, France. pp.187, 10.1117/12.512969 . hal-04514614

HAL Id: hal-04514614

<https://hal.science/hal-04514614>

Submitted on 21 Mar 2024

HAL is a multi-disciplinary open access archive for the deposit and dissemination of scientific research documents, whether they are published or not. The documents may come from teaching and research institutions in France or abroad, or from public or private research centers.

L'archive ouverte pluridisciplinaire **HAL**, est destinée au dépôt et à la diffusion de documents scientifiques de niveau recherche, publiés ou non, émanant des établissements d'enseignement et de recherche français ou étrangers, des laboratoires publics ou privés.

Source follower noise limitations in CMOS active pixel sensors

K.M. Findlater^{1a}, J.M. Vaillant^b, D.J. Baxter^a, C. Augier^b, D. Herauld^b, R.K. Henderson^a, J.E.D. Hurwitz^a, L.A. Grant^a, J-M. Volle^b

^a*STMicroelectronics Imaging Division, 33 Pinkhill, Edinburgh, UK*

^b*STMicroelectronics Central Research and Development, Crolles, Cedex, France*

ABSTRACT

CMOS imagers are commonly employing pinned photodiode pixels and true correlated double sampling to eliminate kTC noise and achieve low noise performance. Low noise performance also depends on optimisation of the readout circuitry. This paper investigates the effect of the pixel source follower transistor on the overall noise performance through several characterization methods. The characterization methods are described, and experimental results are detailed. It is shown that the source follower noise can be the limiting factor of the image sensor and requires optimisation.

Keyword: Active pixel sensors, source follower noise, correlated double sampling

1. INTRODUCTION

Historically, the random noise performance of CMOS image sensors has been limited by the *kTC* (or reset) noise of the photodiode, which is not removed by double data sampling (DDS)¹. The reset noise of the 3T APS has dominated the overall random noise in the image. Typically the random noise of such 3T sensors is not better than 30 electrons (without a severe reduction in the dynamic range). Today, more CMOS imagers are employing a pinned photodiode 4transistor active pixel, which, when combined with correlated double sampling (CDS), eliminates the reset noise.² Therefore other limitations on the imager noise floor come into play. One such limitation is the noise of the pixel source follower transistor, which contains both wide band thermal and low-frequency noise components.³ In this paper, we discuss the extent to which this noise is limiting the random noise floor in our imagers.

This paper is structured as follows. Firstly, some experimental results from a test structure designed to investigate the source follower noise limitation are presented. Then a simple method for determining if the noise is low frequency or thermal noise dominated is introduced. Next, we present the methodology and results from individual pixel noise measurements. These results show that some pixels exhibit a much higher random noise than the average noise for the imager. Then, the variation in measured noise across the manufacturing processing and fabrication facilities is given.

Finally, the discussion of these results and our conclusions are given.

2. TEST STRUCTURE

2.1 Structure design

The test structure (Fig. 1) is included on a revised version of a sensor presented in reference 4. The first revision of the sensor exhibited a higher than expected random noise, despite the use of a pinned photodiode pixel and low-noise column parallel read-out. The test structure duplicates the source follower and access transistor configuration employed in the pixel, but with varying W/L ratio and areas for the source follower transistor.

¹ Keith.Findlater@st.com, phone 44 131 336 6000; fax 44 131 336 6001; www.st.com

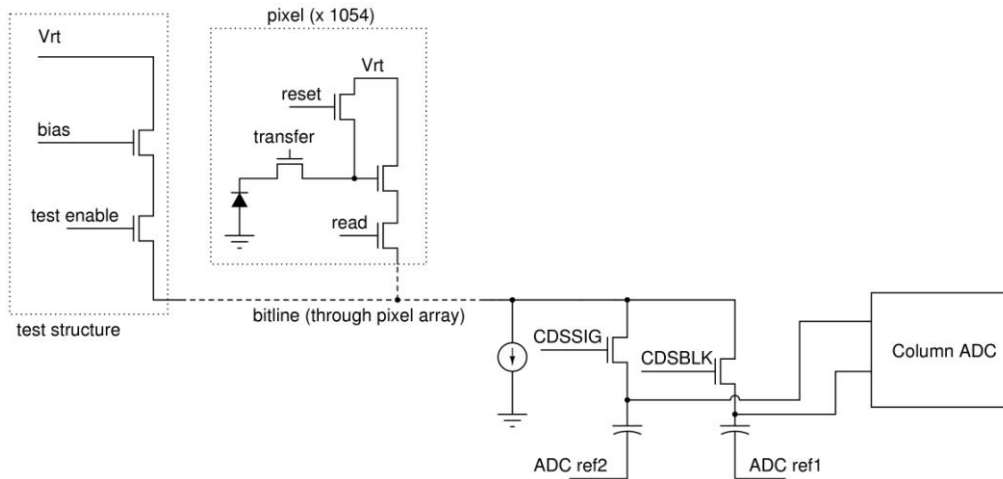


Figure 1 : Schematic of source follower test structure (1 column element)

The structure provides a variety of devices with the same transconductance (and hence thermal noise) but with different size to change the $1/f$ component, and vice versa (Table 1). The structure is connected through the pixel array column lines to the digital read-out circuitry of the sensor and is subject to the same capacitive load as the real pixel source followers.

W (microns)	L (microns)	Transconductance / pixel	Area / pixel
0.8	1.4	0.707	4
1.6	0.7	1	4
3.2	1.4	1	16
0.8	0.35	1	1
3.2	0.35	2	4

Table 1. Source follower test structure device sizes

2.2 Measurement results

Table 2 shows the results of the noise measurements for the structure. The readout noise of the sensor has been subtracted in quadrature from the total noise to give only the source follower component.

W (μm)	L (μm)	Noise μV @ 1.2 μA	Noise μV @ 4.8 μA
0.8	0.35	173	194
0.8	1.4	88	84
1.6	0.7	100	71
3.2	0.35	154	150
3.2	1.4	150	150

Table 2. Measurements of image noise for various W, L and bias current

The minimum device size results in a higher than desired noise, which can be attributed to the higher $1/f$ component. Lower transconductance values with larger area result in low source follower noise due to reduced thermal and $1/f$ components. The results are somewhat contradictory, however, as the lowest noise is achieved using a narrow but long device, rather than simply the largest device. This would suggest that there is a larger effect due to the lower transconductance than is observed in circuit simulation. More investigation of these results is required to draw a firm conclusion.

3. NOISE MEASUREMENT USING VARIABLE CDS TIMING

As well as eliminating pixel reset noise, CDS also attenuates low frequency noise from the pixel, and the period between samples sets the low frequency cut-off of the read-out circuitry^{5,6} (the high frequency cut-off can be reduced by increasing the capacitance on the bitline or reducing the driving transistor transconductance). In our test measurement, which can be performed on our test structure or on the standard pixel, the timing shown in Figure 2 can be used.

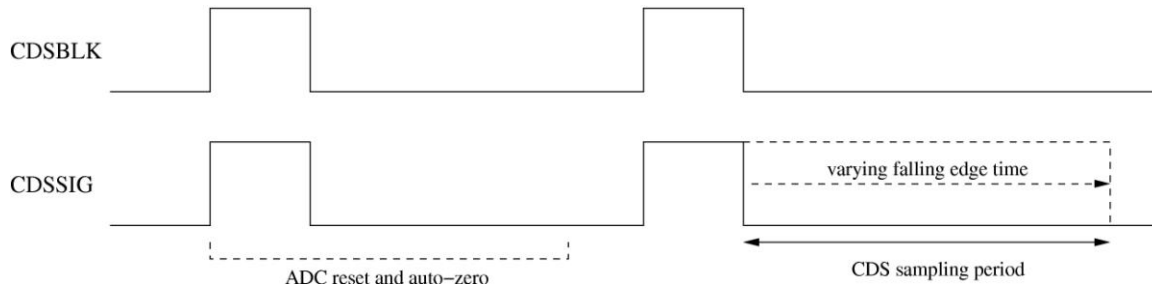


Figure 2 : Variable CDS timing used for source follower measurement

When both CDS pulses are co-incident, both capacitors at the ADC input will contain the same signal: therefore the noise signal from the source follower is eliminated. What noise remains gives a measurement of the read-out noise of the ADC. By increasing the period between the fall of CDSSIG and CDSBLK, a set of noise measurements of an imager can be produced with varying frequency components of the noise eliminated. This measurement method has the advantage that it can be implemented purely through a timing change on the sensor without any extra circuitry.

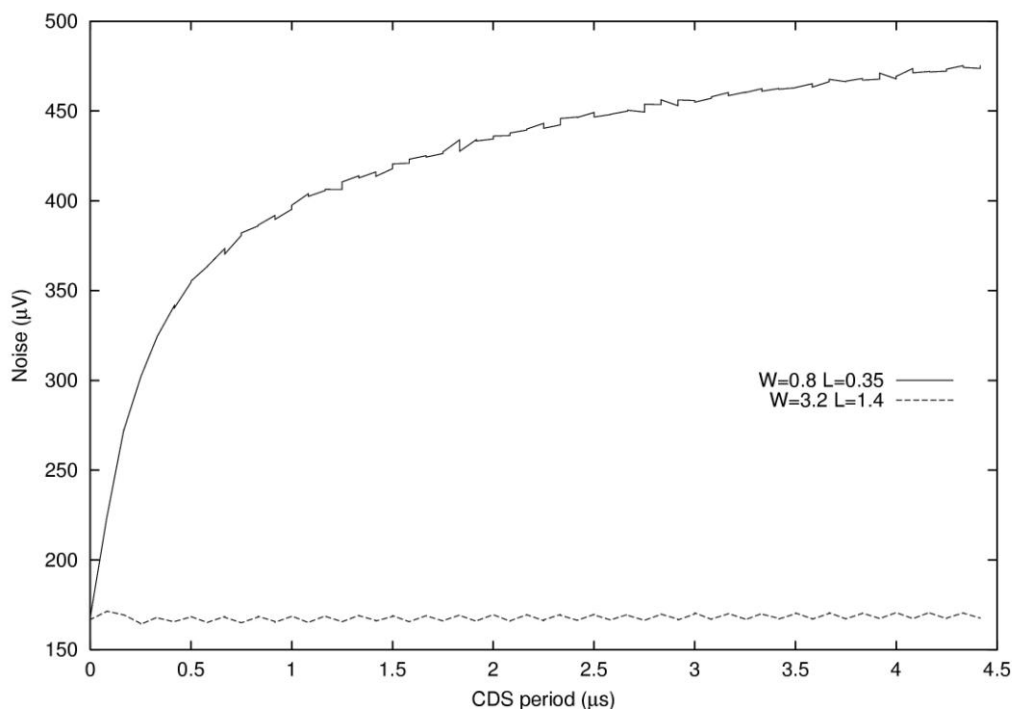


Figure 3 : Measurement of source follower noise with varying CDS sample period

An example measurement using this method is given in Figure 3. When the $1/f$ component of the noise is insignificant and thermal noise dominates (such as in the larger device size) the noise measurement curve is flat over the range of CDS sample periods. Therefore this simple measurement technique can be used to show if $1/f$ or thermal noise limits the sensor noise floor.

4. INDIVIDUAL PIXEL NOISE CALCULATION

4.1 Background

Often, the assumption is made that all pixels in the imaging array have the same average value of noise. Generally, the random noise component of an imager is calculated by subtracting two frames taken at identical conditions on a pixel-

by pixel basis. Any fixed pattern noise is eliminated by the subtraction. Under the assumption that the random noise between the two frames is uncorrelated and of equal magnitude, the noise variance of subtraction result is 2 times that of a single frame.

$$\sigma_{fr1}^2 = \sigma_{fr2}^2 = \frac{\sigma_{sub}^2}{2} \quad (1)$$

where σ_{fr1}^2 and σ_{fr2}^2 are the variances of the first and second frames, and σ_{sub}^2 is the variance of the frame resulting from the subtraction. This method has been used for many years in order to extract important parameters relating to sensor noise performance and conversion gain⁷. However, it does not give any information as to the noise of individual pixels, only the average noise of the whole imager. Plotting the histogram (Figure 4) of the subtracted frame shows that the distribution of the noise is not gaussian, but which pixels are contributing to the non-gaussian result cannot be determined from the simple 2 frame subtraction method.

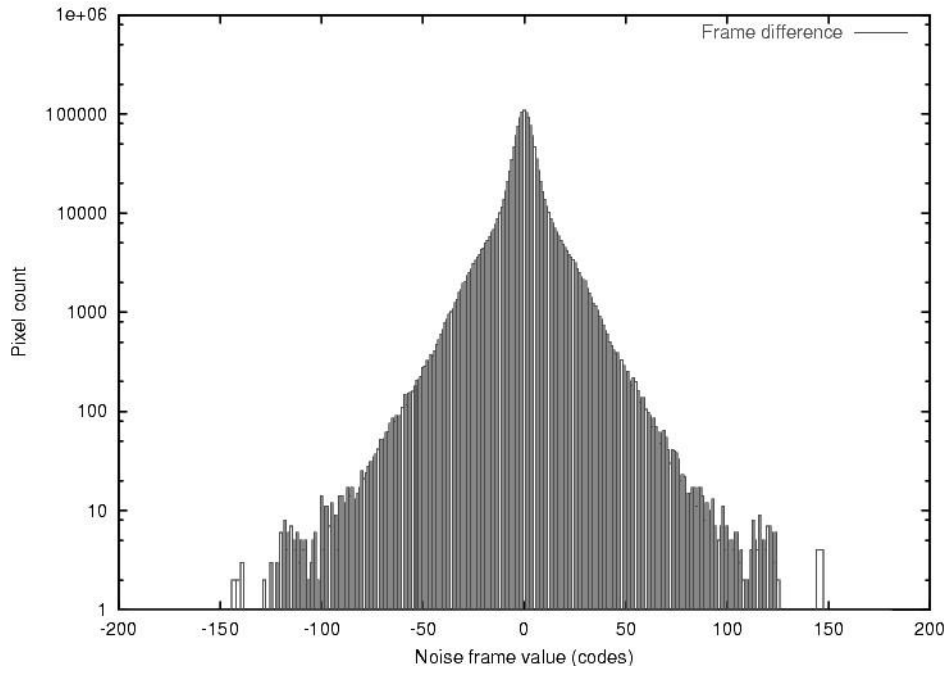


Figure 4 : Histogram of difference frame showing non-gaussian noise distribution

To measure the individual pixel noise, multiple samples from each pixel are taken and the individual pixel variances computed. To achieve a high degree of accuracy several thousand samples can be required, and the storage requirement for this amount of data is very large if the images are captured and the mean and variance computed afterwards. A better approach is shown as follows. Over the number of samples N we accumulate two sums:

$$p_{i,j} = \sum^N X_{i,j} \quad (2)$$

$$q_{i,j} = \sum^N X_{i,j}^2 \quad (3)$$

where $X_{i,j}$ is the pixel output value at row i and column j . After all the images have been acquired the variance of each pixel can be calculated as:

$$\sigma_{i,j}^2 = \frac{1}{N} q_{i,j} - \left(\frac{1}{N} p_{i,j} \right)^2 \quad (3)$$

There is no requirement to store the intermediate results: only two sums need be kept. This considerably decreases the computation time, which can be important if it is necessary to characterize many devices. The average noise σ_{img}^2 for the imager can also be obtained by taking the mean of all the $\sigma_{i,j}^2$ values. Table 3 shows a comparison of the results from the 2 methods for four different devices. In all cases the average noise calculated using both methods is in good agreement.

Device	RMS noise 2 frame method (μV)	RMS noise individual pixel method (μV)
1	260	261
2	251	251
3	232	231
4	181	180

Table 3. Comparison of noise results using the 2 methods

4.2 Results

The result of the individual pixel noise calculation can be displayed as an image as shown in Figure 4. Brighter pixels represent those with a higher noise value. With a source follower device size close to the minimum geometry (e.g. $0.8\mu\text{m}/0.45\mu\text{m}$) a small but significant number of pixels exhibit noise greater much greater than the average. These pixels appear in low-light images where a large analog gain has been applied as time varying defects – switching alternatively from white to black values. They are extremely annoying to eye, especially in colour images where after colour interpolation they can cause erroneous coloured dots to flicker on and off.



Figure 5 : Standard deviation image from a 0.35 micron VGA image sensor

It is desirable therefore to reduce the number of very noisy pixels in the imager. Figure 6 shows the cumulative probability of noisy pixels in a VGA imager for two different source follower lengths. A moderate increase in the source follower length from $0.45\mu\text{m}$ to $0.75\mu\text{m}$ has the effect of reducing the population of noisy pixels with greater than 1mV noise by almost two orders of magnitude. It is usually possible, through pixel layout optimization, to accommodate such an increase in source follower geometry without increasing the pixel size. However, the mean value of the noise is not greatly changed.

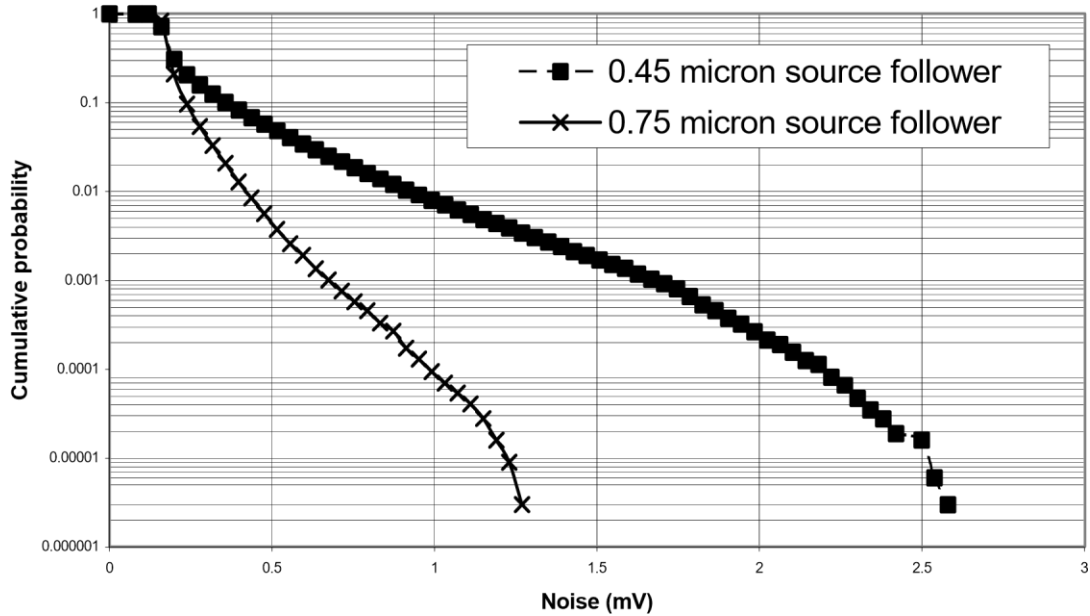


Figure 6 : Cumulative probability plot of pixel noise for 2 different source follower geometries.

Examination of the noisy pixels at the extremes of the distribution has shown that they exhibit random telegraph signal (RTS) noise.^{8,9} The observed flickering on and off of the noise pixels in video sequences is caused by an RTS noise jump between CDS samples of the pixel in question. As imaging technologies migrate to more advanced processes with reduced pixel transistor size, it is likely that this noise source could become a limiting factor in imager noise performance.

5. PROCESS TECHNOLOGY MEASUREMENTS

Source follower noise measurements were also performed on several different silicon lots and technologies to assess the contribution of the pixel source follower noise (Fig. 7). The read-out noise was subtracted from the values in quadrature to give only the noise from the pixel.

It can be seen that there is considerable variation in the source follower noise levels, both between fabs, but also within fabs. The source follower transistor size in both 0.35 μm and 0.18 μm technology was 0.8/0.35 microns. Performance does not seem to deteriorate when moving to 0.18 μm technology though of course normally the transistor size would be reduced. We have also observed a correlation between low threshold voltage source follower transistors and lower noise.

Process development is currently underway to optimise the source follower transistor noise performance.

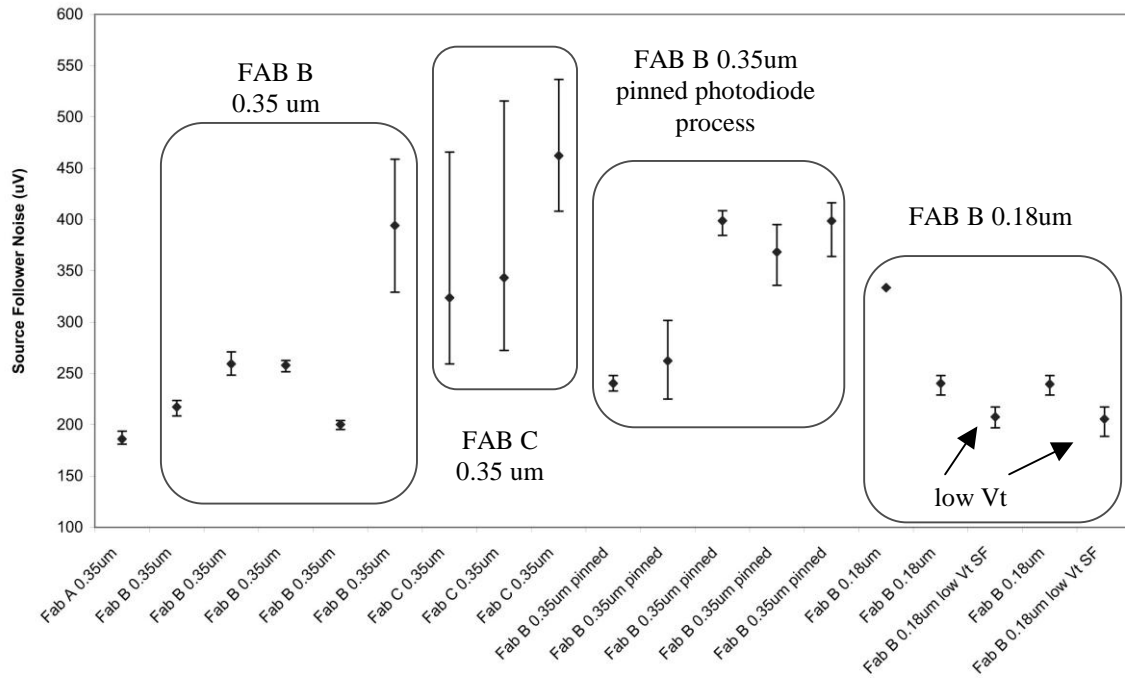


Figure 7 : Source follower noise measurements for lots from various fabrication facilities.

CONCLUSION

In conclusion, pixel source follower noise, especially low-frequency RTS and 1/f components are becoming the limiting factor in imager noise performance. These noise sources have been found to vary considerably both between technologies but also across the same nominal process. The most extreme noisy pixels observed in our imagers were caused by RTS noise. The population of RTS noise dominated pixels can be reduced by a moderate increase in the source follower size. Unfortunately, the use of much larger devices to reduce the 1/f component inside the pixel is not practical due to the strict constraints on pixel size. While circuit design can address the white noise by bandwidth limiting, and can attenuate low frequencies using CDS, process technology optimisation will be required to achieve very low noise pixels with small size.

REFERENCES

1. H. Tian *et al.*, "Analysis of temporal noise in CMOS photodiode active pixel sensor", *IEEE Journal of SolidState Circuits*, vol. 36, no. 1, pp. 92-101, Jan 2001
2. K. Yonemoto *et al.*, "A CMOS image sensor with a simple FPN-reduction technology and a hole accumulation diode", *ISSCC Digest of Technical Papers*, pp. 102-102, Feb 2000
3. J. Janesick, "Lux transfer: CMOS versus CCD", *Proceedings of SPIE*, vol. 4669, Jan 2002
4. K. Findlater *et al.*, "SXGA pinned photodiode CMOS image sensor in 0.35 μ m technology", *ISSCC Digest of Technical Papers*, pp. 218-219, Feb 2003
5. Y. Degerli *et al.*, "Analysis and reduction of signal readout circuitry temporal noise in CMOS image sensors for low-light levels", *IEEE Transactions on Electron Devices*, vol. 47, no.5, pp. 949-962, May 2000
6. R. Gregorian and G. Temes, *Analog MOS Integrated Circuits for Signal Processing*, p.502, John Wiley & Sons, 1986
7. J.R. Janesick *et al.*, "Charge-coupled-device charge-collection efficiency and the photon-transfer technique", *Optical Engineering*, vol. 26, no. 10, pp. 972-980, Oct 1987
8. E. Simoen *et al.*, "Explaining the amplitude of RTS noise in submicrometer MOSFETs", *IEEE Transactions on Electron Devices*, vol. 39, no. 2, pp. 422-429, Feb 1992
9. M. Tsai *et al.*, "The impact of device scaling on the current fluctuations in MOSFETs", *IEEE Transactions on Electron Devices*, vol. 41, no. 11, pp. 2061-2068, Nov 1994